PCCP

ROYAL SOCIETY OF CHEMISTRY

COMMENT

View Article Online
View Journal | View Issue

Cite this: *Phys. Chem. Chem. Phys.*, 2026, **28**, 4967

Comment on "Understanding the infrared spectrum of the protic ionic liquid [DEMA][TfO] by atomistic simulations" by F. Parisi, Y. Chen, K. Wippermann, C. Korte, P. M. Kowalski, M. Eikerling and C. Rodenbücher, *Phys. Chem. Chem. Phys.*, 2024, 26, 28037

John Joo and Allan L. L. East *

Received 23rd June 2025,
Accepted 12th January 2026

DOI: 10.1039/d5cp02379c

rsc.li/pccp

A recent article in this journal (F. Parisi *et al.*, *Phys. Chem. Chem. Phys.*, 2024, **26**, 28037–28045) misassigned the infrared spectrum of liquid diethylmethylammonium triflate (DEMA TfO), a room-temperature ionic liquid. Results from a fresh simulation similar to theirs are shown here, to explain the error and probe the related question of the degree of hydrogen bonding (there does appear to be some). The two peaks in the NH stretch region are due to intensity borrowing (Fermi resonance) from the one NH stretch fundamental by overtone or combination state(s) involving the NH bend.

In 2024, ref. 1 reported results from molecular dynamics simulation of the room-temperature ionic liquid diethylmethylammonium triflate (DEMA TfO), including a calculated infrared spectrum, to revisit the question of the cause of the two high-frequency bands with maxima at 2830 and 3038 cm^{-1} in the IR spectrum.[1–3] Their fresh hypothesis was that the two bands are due to the NH stretch mode in two different ion-pair structural types, to replace a 2010 hypothesis that they are plus-and-minus combinations of NH stretches in a [$DEMA^+$·TfO^-·$DEMA^+$] triple ion.[2] However, (i) their computed spectrum from the simulation shows 3 peaks (not the 2 seen experimentally), and (ii) they observed very continuous distributions, of both vibrational density-of-states in their Fig. 7 and NH–O angles in their Fig. 10, which appear to contradict rather than support their hypothesis of multiple structural types.

It would be more definitive to probe distributions of NH bond lengths, rather than NH–O angles, when testing a hypothesis that two clearly separated infrared bands in the NH stretch region are due to the NH bond in two distinct environments. Some exemplary quantum-chemistry harmonic-oscillator IR spectra[4] are shown in Fig. 1 to demonstrate the strong dependence of the NH stretch frequency upon proximity of triflate ion. The frequency depends linearly on the N–H bond length (rather than the H···O hydrogen-bond distance, see Fig. 2). This means that their hypothesis, that the two distinct peaks represent two hydrogen bond types, requires two distinct peaks in the N–H bond-length distribution plots from simulation.

We then performed our own simulation of this liquid,[6] running it for 37 000 femtosecond timesteps, monitoring the eight NH bond lengths. Our starting positions had the NH bonds aimed at the CF_3 end of the triflate ($CF_3SO_3^-$) ions. Within ~3000 fs each NH bond found an SO_3 group, adopting one (not two) preferred hydrogen-bonded orientation (Fig. 3). Over time, the pair distribution functions (histograms) of N-to-H distances for each of the eight *r*(N–H) covalent bonds evolved towards a single-peak distribution (Fig. 4), demonstrating that two distinct N–H covalent bond lengths do not exist in this liquid in this simulation. Ref. 1, had they made such N–H plots from their simulations, would likely have observed the same. Thus, such simulations refute the hypothesis that two distinct N–H stretch fundamentals could arise from this liquid. The multiple peaks, in both the experimental and AIMD infrared spectra, are due to some other phenomena.

The nature of this observed (simulated) hydrogen bond is of interest. Triflate-based ionic liquids do not suffer terribly from limited ionicity (inhibited conductivity) as carboxylic-acid-based ones sometimes do.[11–13] The simulation, however, shows apparent ion pairing. Fig. 3 shows that there is a particular and consistent SO_3–HN hydrogen-bonded geometric arrangement, with three unique NH–O distances: the classic 1.8 Å hydrogen bond, plus 3 Å and 4 Å to the other SO_3 oxygen atoms. Each hydrogen bond was seen to exist for several picoseconds, perhaps 10 ps on average, before undergoing a quick (~10 fs) hop, of an NH unit from O to O. Such hops occurred to an O of

Department of Chemistry and Biochemistry, University of Regina, Regina, SK, Canada S4S 0A2. E-mail: allan.east@uregina.ca

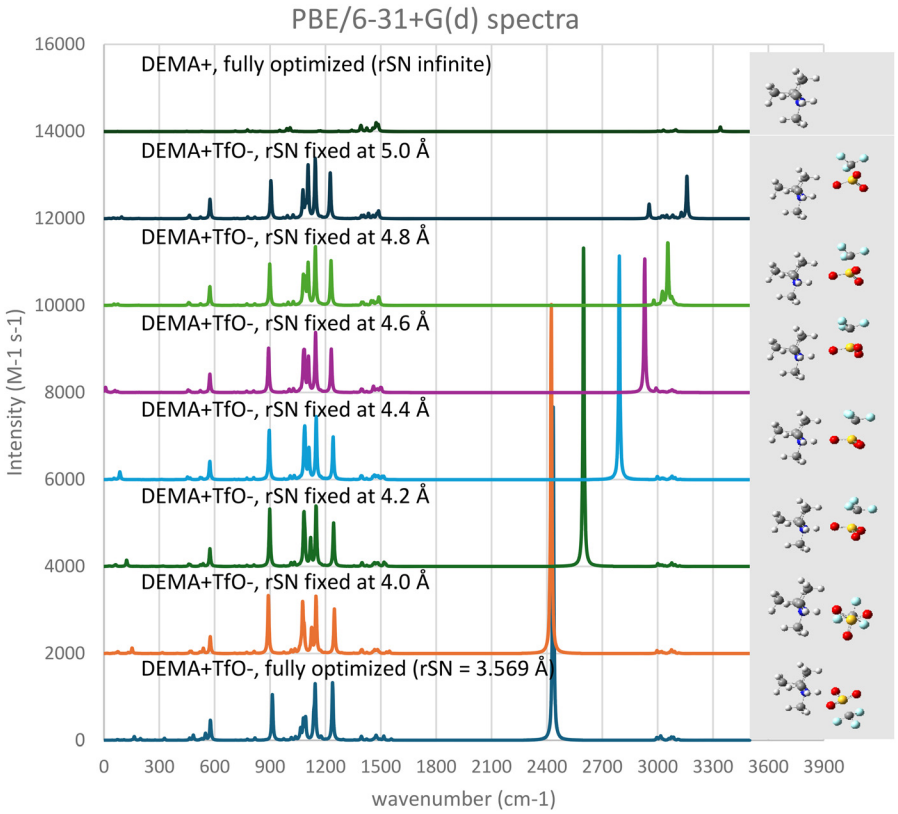

Fig. 1 Predicted (density-functional-theory) gas-phase IR spectra (double harmonic approximation) from restricted optimizations of ion pairs, varying the cation N to anion S distance, demonstrating the migration of the NH stretch peak from 2400 to 3300 cm^{-1} with increasing ion-pair distance.

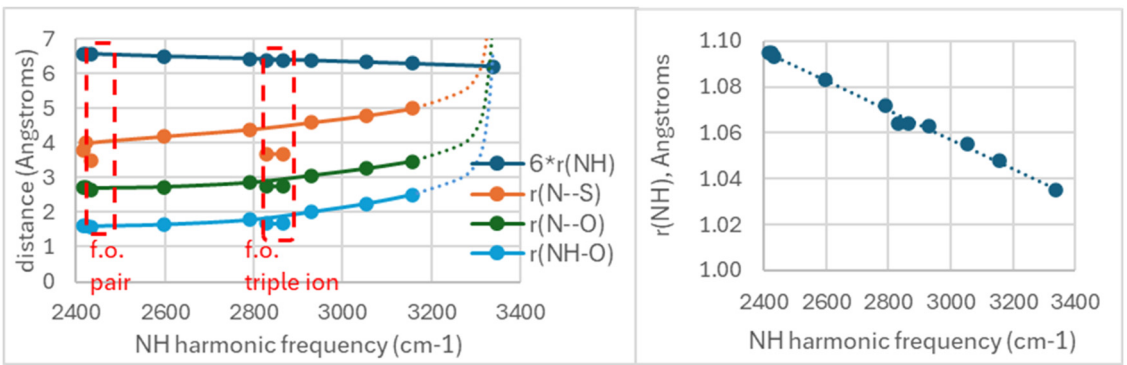

Fig. 2 Correlating the predicted NH vibrational (harmonic) frequency with various interatomic distances in the structures used for their generation. Includes all structures from Fig. 1 plus the two NH stretch frequencies from the fully optimized triple-ion [$DEMA^+ \cdot TfO^- \cdot DEMA^+$]. The hydrogen-bond distance is *r*(NH–O) in the plot.

the same triflate (*e.g.* t = 14 000 fs, upper plot) or from triflate to triflate (t = 29 000 fs, lower plot, forming a [$DEMA^+ \cdot TfO^- \cdot DEMA^+$] triple ion in this case). Note, however, that a hydrogen bond average lifetime of 10 ps between hops might be considered low, indicative of a weak hydrogen bond, such that with the addition of even a slight electric field (conductivity measurements), the hydrogen bond is perhaps easily overcome, effecting only limited inhibition to the ability of $DEMA^+$ and TfO^- ions to individually conduct current.

The correct explanation for the two peaks in the NH-stretch region of the infrared spectrum, at 2830 and 3080 cm^{-1}, is a Fermi resonance (intensity borrowing) by an overtone or combination band involving the NH bend mode. Such a phenomenon has been observed in alkylammonium salt crystals[14–18] and even in polynucleotides DNA and RNA.[19] Particularly convincing here would be the reports by Kuo and co-workers in the gas phase, studying NH–O in particular, with a series of the forms $XYZNH^+ \cdot OH_2$ (varying the amine XYZN)[20] and $Et_3NH^+ \cdot OHR$

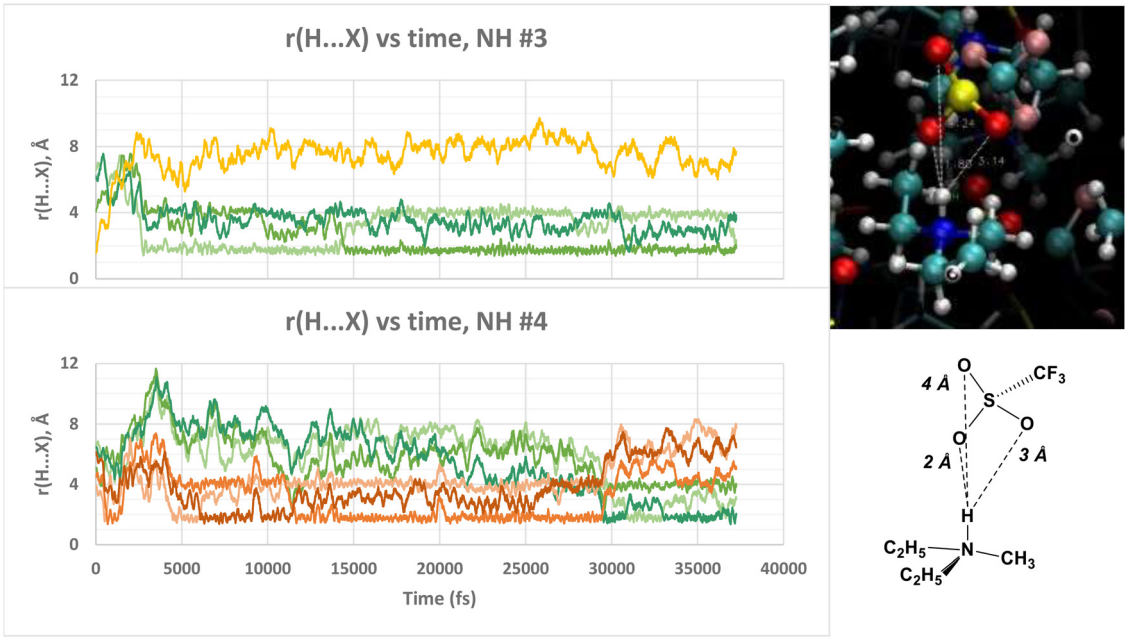

Fig. 3 Plots of the distances from the H atom of N–H bond #3 (upper) and #4 (lower), to (i) its initially nearest neighbour (an F atom of a triflate CF_3 group, yellow), (ii) each of the three O atoms of triflate ion #1 (green), (iii) each of the three O atoms of triflate ion #2 (orange), demonstrating the nature of the hydrogen bond in the ion pair. Note the steady nature of the hydrogen bond at $r(H\cdots O) \approx 1.8$ Å, the hops from O to O within a triflate (*e.g.* $t = 14\,000$ fs, upper plot) and from triflate to triflate ($t = 29\,000$ fs, lower plot), and the negligible time the H spends bridging two O's when hopping from O to O. Upper right: a typical ion-pair snapshot (VMD graphics software[10]). Lower right: relating the snapshot to the three unique H···O distances near 2, 3, and 4 Å in the graphs.

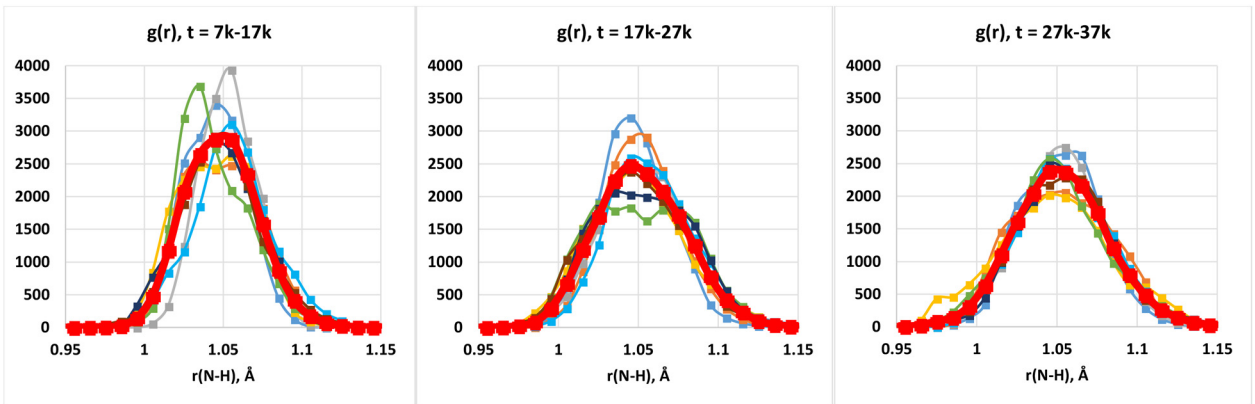

Fig. 4 Plots of the radial distribution function $g(r\mathrm{NH})$, for each of the eight NH bonds in the simulation (thin lines) as well as their average (thick line), showing their evolution to a single-peak distribution.

(varying R),[21] showing an excellent match (their $Me_3NH^+\cdot OH_2$ case) of the two bands seen in liquid DEMA TfO. A Fermi-resonance splitting (three or four bands, split across a 150 cm^{-1} range) has also been identified with OH–N hydrogen bonds, in nonionic XYZN·HOH gas-phase pairs.[22,23]

Conflicts of interest

There are no conflicts to declare.

Data availability

Data can be reproduced from information provided, but input and output files can also be requested from the corresponding author upon request.

Acknowledgements

The work was supported by the Natural Sciences and Engineering Research Council (DDG-2023-00008). The simulation was

performed on Canada's Digital Alliance supercomputers Graham and Cedar, enabled in part by support provided by the Digital Research Alliance of Canada (https://alliancecan.ca), financially supported by the Canada Foundation for Innovation.

References

1 F. Parisi, Y. Chen, K. Wippermann, C. Korte, P. M. Kowalski, M. Eikerling and C. Rodenbücher, *Phys. Chem. Chem. Phys.*, 2024, **26**, 28037–28045.
2 K. Mori, S. Hashimoto, T. Yuzuri and K. Sakakibara, *Bull. Chem. Soc. Jpn.*, 2010, **83**, 328–334.
3 M. S. Miran, T. Yasuda, M. A. B. H. Susan, K. Dokko and M. Watanabe, *RSC Adv.*, 2013, **3**, 4141–4144.
4 Spectra in Fig. 1 computed with the Gaussian09 quantum-chemistry software[5] at the PBE/6-31+G(d) level of theory, using geometries from restricted optimization, fixing the N–S distance at various values and optimizing all other internal coordinates.
5 Gaussian09: M. J. Frisch, *et al.*, *Gaussian09, Rev. C.01*, Gaussian, Inc., Wallingford CT, USA.
6 Simulation performed with the VASP *ab initio* molecular dynamics software[7] with the same approximations as used before (the GGA = 91 (PW91), IVDW = 12 level of density-functional theory for the forces on atoms, default precision, Nosé heat bath),[8] using eight $DEMA^+$ and eight TfO^- ions in a rectangular-prism periodically replicated simulation cell (18.097 × 15.105 × 9.012 Å, to match known[9] density 1.284 g cm^{-3}), and a temperature set to 298 K.
7 VASP: G. Kresse, *et al.*, *Vienna Ab-initio Simulation Package, rev. 5.4.4*, VASP Software GmbH, Berggasse 21/14, A-1090, Vienna, Austria.
8 A. A. Mukadam, N. P. Aravindakshan and A. L. L. East, *Phys. Chem. Chem. Phys.*, 2020, **22**, 7119–7125.
9 T. Yasuda, H. Kinoshita, M. S. Miran, S. Tsuzuki and M. Watanabe, *J. Chem. Eng. Data*, 2013, **58**, 2724–2732.
10 W. Humphrey, A. Dalke and K. Schulten, *J. Mol. Graphics*, 1996, **14**, 33–38.
11 W. Xu, E. I. Cooper and C. A. Angell, *J. Phys. Chem. B*, 2003, **107**, 6170–6178.
12 K. Ueno, H. Tokuda and M. Watanabe, *Phys. Chem. Chem. Phys.*, 2010, **12**, 1649–1658.
13 D. O. Klapatiuk, S. L. Waugh, A. A. Mukadam and A. L. L. East, *J. Chem. Phys.*, 2023, **158**, 034507.
14 R. D. Waldron, *J. Chem. Phys.*, 1953, **21**, 734–741.
15 C. Brissette and C. Sandorfy, *Can. J. Chem.*, 1960, **38**, 34–44.
16 O. Knop, T. S. Cameron, M. A. James and M. Falk, *Can. J. Chem.*, 1981, **59**, 2550–2555.
17 O. Knop, T. S. Cameron, M. A. James and M. Falk, *Can. J. Chem.*, 1983, **61**, 1620–1646.
18 M. A. James, T. S. Cameron, O. Knop, M. Neuman and M. Falk, *Can. J. Chem.*, 1985, **63**, 1750–1758.
19 G. Zundel, W. D. Lubos and K. Kölkenbeck, *Can. J. Chem.*, 1971, **49**, 3795–3798.
20 C.-K. Lin, R. Shishido, Q.-R. Huang, A. Fujii and J.-L. Kuo, *Phys. Chem. Chem. Phys.*, 2020, **22**, 22035–22046.
21 Q.-R. Huang, R. Shishido, C.-K. Lin, C.-W. Tsai, J. A. Tan, A. Fujii and J.-L. Kuo, *Angew. Chem., Int. Ed.*, 2021, **60**, 1936–1941.
22 E. Lwin, T. L. Fischer and M. A. Suhm, *J. Phys. Chem. Lett.*, 2023, **14**, 10194–10199.
23 E. Lwin, N. O. B. Lüttschwager and M. A. Suhm, *Phys. Chem. Chem. Phys.*, 2025, **27**, 5808–5820.

